RSC Advances

ROYAL SOCIETY OF CHEMISTRY

www.rsc.org/advances

RCS Advances

RSCPublishing

ARTICLE

Elaboration of Poly(lactic-acid)/Halloysite nanocomposites by means of water assisted extrusion: Structure, Mechanical properties and Fire performance

Cite this: DOI: 10.1039/xoxxoooooox

Received ooth January 2012,
Accepted ooth January 2012

DOI: 10.1039/xoxxoooooox

www.rsc.org/

G. Stoclet[a]*, M. Sclavons[b], B. Lecouvet[c], J. Devaux[b], P. Van Velthem[b], A. Boborodea[d], S. Bourbigot[a], N. Sallem-Idrissi[b]

Poly(lactic acid) (PLA)/Halloysite nanotubes (HNTs) nanocomposites were prepared using a water assisted extrusion process. Morphology, structure, thermomechanical properties and fire performance of these nanocomposites were compared to those obtained in the case of nanocomposites elaborated via conventional extrusion process. Whatever the elaboration route used, mechanical tests indicate that HNTs have a reinforcing effect ascribed to the dispersion, at least partial, of the HNTs into the PLA matrix. Differential Scanning Calorimetry also shows that HNTs infers on the PLA crystallization and play the role of nucleating agent. Moreover cone calorimeter experiments show a drastic improvement of the reaction to fire of PLA when HNTs are added, especially for high filler contents. This improvement arises from the fact that HNTs induce the formation of a protective inorganic layer at the surface of the sample. As main results of this study, it has been shown that water assisted extrusion not only induced a better dispersion of the HNTs into the matrix but also that this process prevents polymer degradation during the extrusion. This unusual effect has been ascribed to a barrier effect of the water molecules that preferentially locate at the HNTs-matrix interface. Even if not fully explained, it could be ascribed to a decrease of local shear levels (mechanochemical effect) and/or to a decrease of catalytic effect of the HNTs surface (chemical effect). Consequently this study reveals that water-assisted extrusion is a reliable route to prepare PLA/Halloysite nanocomposites with enhanced properties.

Introduction

Polylactic acid (PLA) is an aliphatic polyester issued from renewable resources such as sweet corns and sugar beets. PLA exhibits many interesting physico-chemical properties such as high strength, biocompatibility, thermoplastic grease and oil resistance, and excellent aroma barrier [1,2,3,4]. Consequently this polymer is foreseen as a good candidate for the replacement of petroleum based polymer in some applications. However this polymer suffers from a lack of properties for an enlargement of its application fields. Particularly PLA exhibits poor fire resistance properties and a lower elastic modulus than Poly(ethylene terephthalate) (PET) or Poly(styrene) (PS)[5]. One of the ways to outclass this lack of properties is the elaboration of nanocomposites. This technology, consisting in incorporating into the polymer matrix inorganic fillers having at least one nanometric size, has known an increasing interest since the pioneer works carried out by the Toyota's research group that has revealed that the incorporation of only a few percent of nanofiller can strongly improve the materials properties[6,7,8,9]. This strategy has been largely applied to the case of PLA in the past years and there are presently a large number of studies devoted to the elaboration and characterization of PLA nanocomposites.

Up to now most of the elaborated nanocomposites are based on fillers, organically modified or not, having a platelet like shape such as layered silicates. The reported studies indicate that the incorporation of MMT into PLA can increase its properties such as the mechanical or permeability ones. For example Sinha Ray et al. have shown that the flexural modulus of PLA can be increased from 17% to 27%, depending on the surfactant used, when 4wt% of organomodified Montmorillonite or mica are added[10]. In the same way Chiu et al. show that adding 7wt% of carbon nanotube increases the elastic modulus by 20%[11]. More generally, a review of the works dealing with the elaboration and the characterization of polymer nanocomposites reveals that the degree of properties improvement strongly depends on both the achieved dispersion state of the filler and, second, of the affinity between the polymer and the matrix. Particularly high dispersion state and strong affinity between the filler and the matrix will lead to the highest properties enhancement.

In addition to the improvement of mechanical properties previously discussed, the elaboration of nanocomposites can also drastically enhance its fire performance. For this purpose fillers, that act as flame retardant, are currently used as they may involve a significant improvement of the fire retardation properties[12,13,14]. Regarding other kinds of fillers, recent studies have shown that filling PLA with clays or carbon nanotubes can also improve its fire resistance properties. For example Murariu et al. report a decrease of 35% of the peak of Heat Release Rate (pHRR) accompanied by the formation of a char when 3wt% of Cloisite30B is added to PLA[15] and a decrease by 30% when 6wt% of expandable graphite is added[16].

Recently, a "new type" of inorganic filler emerged and is increasingly studied: the Halloysite nanotubes (HNTs). Halloysite is a naturally occurring aluminosilicate ($Al_2Si_2O_5(OH)_4.2H_2O$) with a predominantly hollow tubular structure mined from natural deposits in countries such as America, China, New Zealand, France and Belgium[17]. Halloysite exhibits high elastic modulus[18] and unique surface chemical property due to the multi-layer structure with only a few hydroxyl groups located on the surface of the nanotubes[19]. As compared to other layered silicates, halloysite can thus be easily dispersed in a non-polar polymer matrix like polypropylene (PP) due to weak secondary interactions among the nanotubes[20]. Moreover the high polarity of the polyamide (PA) matrix enables to obtain efficient dispersion of the nanotubes by formation of H-bonds between polymer and filler. During the past years an increasing number of research groups have studied the elaboration and characterization of polymer nanocomposites based on HNTs[21,22,23,24]. Most of the publications were devoted to the elaboration and study of mechanical properties of polymer/halloysite composites. Besides it was reported a significant improvement of tensile strength, tensile modulus and elongation at break at low HNTs content[19,23,24,25,26].

Recently, several studies have been focused on the elaboration and characterization of PLA based HNTs nanocomposites. All these works report that adding HNTs into PLA involves an enhancement of mechanical properties and thermal stability[27,28,29] while thermal properties such as glass transition of crystallization kinetics remains mostly unaffected. For example, Wu et al.[30] reported an increase of about 20% of the tensile modulus when 7wt% of HNTs is added. The reinforcing effect was correlated to the high aspect ratio, excellent

dispersion and high intrinsic stiffness of the nanotubes. These works also indicate that a better dispersion degree and consequently a higher properties enhancement was achieved with the use of surface treated HNTs[30,32,31]. Finally, regarding the effect of HNTs on the barrier properties, reported results indicate a slight enhancement of water barrier and gas properties[32,33].

In addition to the reinforcing effect, the incorporation of Halloysite may also improve the fire retardation properties[34]. For example Marney et al. have shown, in the case of Polyamide 6, that halloysite nanotubes influence the fire performance due to the fact that a thermal insulation barrier is developed at the surface of the composite during the combustion. This barrier acted to retard burning (high decrease of heat release rate) without stopping it and more than doubled the total burning time (to be compared to the slow burning of candle). The same behavior was observed by Lecouvet et al. on PP/Halloysite nanocomposites[35]. In their study, authors show that the incorporation of HNTs into polypropylene (PP) can drastically enhance the fire properties of PP only if HNTs are well dispersed. To achieve this goal they use the water assisted extrusion route that allow getting access to a better dispersion of the HNTs as compared to conventional routes[36]. The synergistic effect of injecting water during the extrusion process on the dispersion degree of the filler has already been demonstrated, mainly in the case of nanocomposites based on polyamides[37,38,39].

Consequently, in this study, it is proposed to elaborate and to characterize PLA nanocomposites based on HNTs using the water assisted extrusion process. Water assisted extrusion process has been used with the aim of improving the dispersion degree of the HNTs into the PLA matrix. For the sake of comparison, nanocomposites elaborated using a conventional extrusion process, i.e. without water injection, were also studied. On the one hand a particular attention has been paid to finely characterize the morphology and the structure of the elaborated nanocomposites. On the other hand mechanical, rheological, fire properties as well as thermal stability of PLA were studied in order to give the structure property relationships of these materials. The influence of the HNTs content has also been studied.

Experimental

Materials & Elaboration

The PLA investigated in this work, containing 4.3mol% of D-isomer units (grade 4042D), was purchased from Natureworks (USA). Halloysite nanotubes were purchased from Sigma Aldrich (Germany) and used without any chemical modification. Typical specific surface area of this halloysite is 64 m²/g; cation exchange capacity of 8 meq/g; pore volume of 1.25 ml/g; and specific gravity of 2.53 g/cm3.

The PLA nanocomposites were elaborated by melt blending in a co-rotating twin-screw extruder Coperion Mega Compounder WP ZSK25 (L/D= 40). Water, when used, was pumped into the extruder in the high compression zone. The special design of the screw allows the pressure to increase up to 125 bars in this zone which prevents water evaporation. The water is degassed in the transport zone and fully removed using a vacuum pump. The processing temperature, the throughput (TP), the screws speed (SP) and the water injection rate (W) were adapted to the experience. A more detailed description of this process is available elsewhere[40,41]. The elaboration conditions used in this study are listed in table I.

Temperature (°C)	Material throughput (kg/h)	Screws speed (rpm)	Water input (ml/min)	Clay throughput (wt%)
180°C	7	300	0 & 50	0 , 4 , 8 & 17

Table I : Elaboration conditions used

Nanocomposites filled with HNTs contents varying from 0% to 17wt% have been elaborated. Structural and morphological characterizations were performed on the as extruded pellets. Mechanical and fire retardation properties characterizations were carried out on compression molded samples from 0.5mm thick and 3mm sheets respectively, molded at 190°C under 90 bars. Prior to compression molding, pellets were dried at 50°C under vacuum during 12h. For the sake of clarity, samples will be denoted PLA-HX-W where X represents the weight content percentage of Halloysite and W the fact that water was injected during the extrusion.

Molecular weight determination

Average molecular weight (Mw) of both the pellets and extruded materials were measured by Size Exclusion Chromatography (SEC). A waters 2695 Separation Module equipped with a Waters Filter guard column and three PLgel 5µm (100Å, 10^3Å and 10^4Å pore sizes) 300x7.5mm² columns as well as a differential refractometer, were used for Mw determination. Tetrahydrofuran (THF, Biosolve, stabilized with butylhydroxytoluene) was used as mobile phase at a flow rate of 0.8 ml/min. SEC calibration was done using polystyrene (PS) standards and using universal calibration standards. Data acquisitions were performed by Waters Millenium software. Prior to analysis, solutions were filtered through 0.45µm filters (Millex FH – Millipore).

Structural characterization

Wide-Angle X-ray Scattering (WAXS) analyses were carried out using a Genix micro-source equipment (Xenocs, France) operating at 50 kV and 1 mA. The Cu Kα radiation used (λ = 1.54 Å) was selected with a curved mirror monochromator (Fox2D-12Inf, Xenocs). Analyses were carried out on the 0.5mm thick solid molded samples in transmission mode. WAXS patterns were recorded on a 2D CCD VHR camera (Photonic science), the distance between sample and detector (D) being set at 7cm for WAXS. The working distance was calibrated using silver behenate as standard. Standard corrections such as distortion, dark current subtraction and background correction were applied before analysis. The 2D WAXS patterns obtained were then azimuthally integrated using the fit2D software.

Morphology characterization

Samples morphologies and dispersion degree of the HNTs into the PLA matrix were characterized at different scale levels by means of Optical Microscopy (OM), Scanning Electronic Microscopy (SEM) and Transmission Electronic Microscopy (TEM).

OM micrographs were obtained by means of a binocular optical microscope Olympus AX41 equipped with a numerical camera Olympus DP12. Examined area of the produced composites was prepared from a ±0.5 mm thin film cut from the elaborated pellets using a razor blade. Micrographs of the samples were taken under magnitude of 10 to provide an actual visual aspect of the samples. Clay dispersion and exfoliation degree were examined by means of SEM and TEM. SEM analyses were carried out on cryofractured samples using a LEO 982 (Zeiss) SEM operating at 1kV. The TEM micrographs were recorded using a CM30 (Phillips) transmission electron microscope operating at 300 kV. Analyzed samples were thin films, having of thickness of approximately 70nm, microtomed from bulk samples at room temperature using a Leica Reichert FCS microtome and collected on a 300µm² mesh copper grid.

Thermal properties

Thermal properties were determined by means of Differential Scanning Calorimetry (DSC) on a Pyris Diamond apparatus from Perkin Elmer. The 10mg samples, placed into aluminium pans, were scanned at a heating rate of 10°C/min under nitrogen gas flow. The temperature and heat flow scales were calibrated using a high purity indium sample according to standard procedures. The crystalline weight fraction was computed from the enthalpy of the melting exotherm using the specific enthalpy of fusion of the perfect crystal, $\Delta Hm°=94J/g$[42] for PLA.

The thermal stability of the materials was studied by Thermo Gravimetric Analysis (TGA). The analyses were performed using a TGA/SDTA 851e (Mettler-Toledo, Switzerland). Samples of about 13mg were heated from room temperature to 600 °C at a constant heating rate of 10°C/min under nitrogen atmosphere with a flow rate of 100 ml/min. TGA results are presented as temperatures at 10% weight loss (T10). This temperature is usually considered as the onset of the degradation.

Mechanical behavior

Uniaxial tensile tests were carried out using an Instron machine Model 4466. The dumbbell specimens having 22 mm and 5 mm in gauge length and width were cut out from the 0.2 mm thick sheets and strained at a constant crosshead speed of 50 mm/min, i.e. an initial strain rate $\dot{\varepsilon} = 3.10^{-2}\ s^{-1}$. Five specimens were tested for each blend and experimental condition. The yield stress, σ_y, is defined at the stress overshoot prior to necking at room temperature (RT). The strain at break, ε_{break}, is defined as the ratio of the sample length at break to the initial gauge length of the sample.

Fire properties

The cone calorimeter tests were carried out using a FTT (Fire Testing Technology) Mass Loss Calorimeter following the procedure defined in ASTM E 906. The equipment is similar to the one used in oxygen consumption cone calorimetry. The only difference is the use of a thermopile at the top of the chimney to measure the heat release rate (HRR) instead of employing the oxygen consumption principle. The specimens (100x100x3 mm^3) were irradiated in a horizontal position by an external flux of 50kW/m² and the flame ignition was initiated using a spark igniter. The flammability parameters considered in this study are: heat release rate (HRR), peak of heat release rate (PHRR), total heat release (THR), residue and the time to ignition (TTI). The cone data reported in this paper are based on the average of three replicated experiments and are reproducible with variation less than 10%.

Results

Molecular weight determination

The thermo-mechanical properties of PLA are highly sensitive to its molecular weight[43]. Thus the influence of both the processing conditions used and the HNTs content on the molecular weight were studied. Figure 1 depicts the evolution of the weight average molecular weight (Mw) as a function of the clay content for samples elaborated with and without water injection during the extrusion.

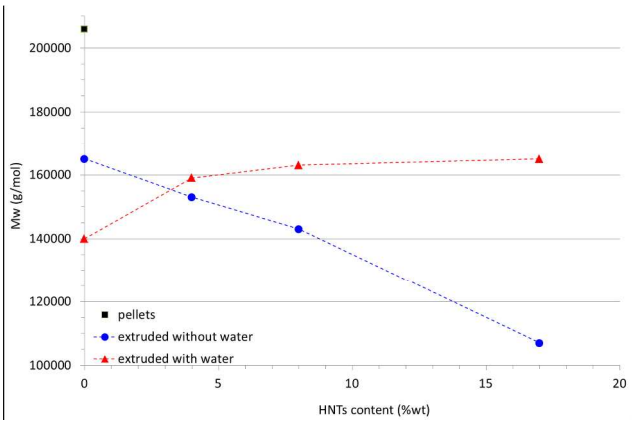

Figure 1: Molecular weight as a function of both filler content for PLA nanocomposites extruded with and without water injection.

Regarding unfilled materials, it appears that extruded samples exhibit a lower Mw as compared to the PLA pellets (Mw ≈ 205 kg/mol). This decrease of Mw is explained by thermal and/or mechanical degradation of PLA that induces chain scissions during the extrusion process[44]. Worth noting is that this degradation is more pronounced in the case of water assisted extrusion indicating a negative effect of adding water in the case of unfilled PLA. This stronger decrease of Mw probably arises from a hydrolysis of the PLA chains by the water molecules.

Regarding the HNTs filled materials it appears on the one hand that in the case of conventional extrusion, Mw steadily decreases with increasing the HNTs content. This result ascribed to an increase of thermomechanical degradation in the presence of filler has ever been reported and ascribed to catalytically effect of the clay[45,46] and also probably arises from a local overheating induce by shear concentrations. On the other hand, in the case of water assisted extrusion, it appears surprisingly that i) Mw is not affected by the presence of the HNTs and ii) Mw for the filled materials is higher than the one of the unfilled sample. This result is unusual as much as PLA is known to suffer from hydrolytic degradation[47] and also due to the fact that, as observed in the case of conventional extrusion, the presence of HNTs also promotes the polymer degradation. This point will be discussed later in the manuscript.

Morphological & structural characterizations

A key parameter that governs the thermo-mechanical properties of polymer nanocomposites is the dispersion state of the filler. In order to assess the presence of agglomerates, the nanocomposites were first observed by means of Optical Microscopy (OM). Characteristic pictures of the morphology are reported in figure 2.

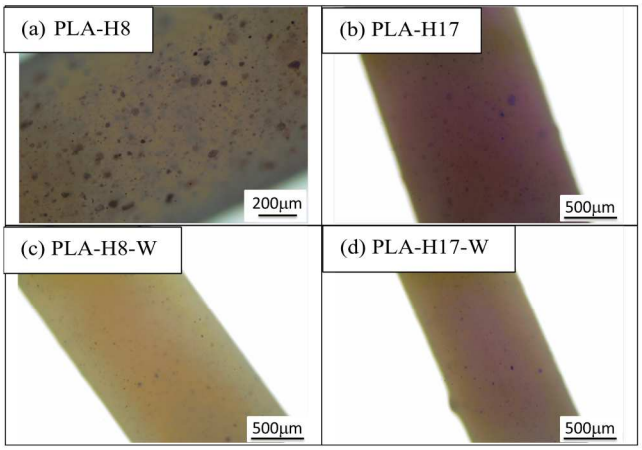

Figure 2: Optical micrographs of (a) PLA-H8, (b) PLA-H17, (c) PLA-H8-W and (d) PLA-H17-W

Regarding the nanocomposites having a HNTs content of 4wt%, no aggregates were detected either water was injected or not during the extrusion (pictures not shown here). This may suggest that a good dispersion state is achieved in both cases. For higher HNTs contents, OM micrographs indicate that some aggregates are still present into the material. Worth noticing is that the number of visible aggregates having micronic sizes is fairly lower in the case of the nanocomposites extruded with water. To support this point, the morphology of the nanocomposites was observed by SEM.

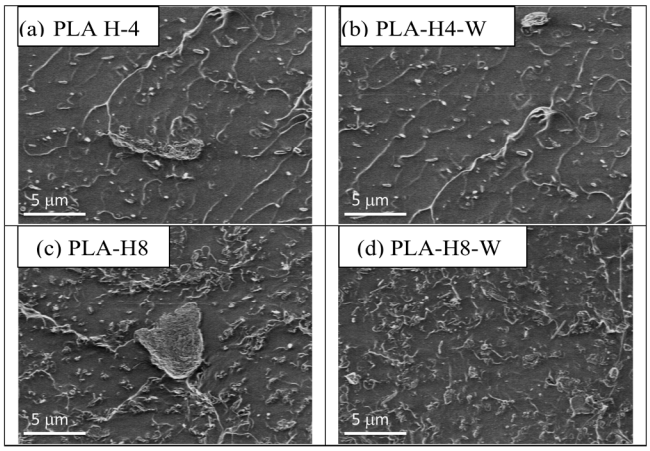

Figure 3: SEM observations of (a) PLA-H4, (b) PLA-H4-W, (c) PLA-H8 and (d) PLA-H8-W nanocomposites

SEM micrographs depicted in figure 3 show the morphology of PLA nanocomposites at low (4wt%) and intermediate (8wt%) HNTs loadings. A homogeneous distribution of the clay is achieved for PLA-H4 systems, whatever the processing route (Fig. 3a and 3b). Most of the tubes (i.e. white spots) are well individualized into the organic matrix without any significant trace of aggregation. At 8wt% HNTs, a heterogeneous structure is observed in nanocomposites elaborated by classical extrusion due to the presence of more aggregates (Fig. 3c). Interestingly, the use of water during melt compounding improves the nanoscale dispersion of halloysite as revealed by the higher density of single nanotubes in PLA-H8-W nanocomposite (Fig. 3d) as compared to the reference system (Fig. 3c).

Finally to get a local representation of the nanocomposites morphologies, TEM analyses were carried out with the aim of finely characterizing the dispersion degree of the HNTs as a function of both the clay content and the process used. Micrographs representative of the microstructure of the nanocomposites having clay contents of 8 and 17wt% elaborated with and without water injection are reported in figure 4.

TEM analyses confirm the previous SEM and OM results. To summarize, while at 4wt% of clay the HNTs are fully exfoliated, some aggregates are still presents at higher clay contents. Moreover, the beneficial effect of injecting water during the extrusion is clearly highlighted as the exfoliation degree at clay contents above 4wt% is fairly higher for the water-assisted extruded nanocomposites.

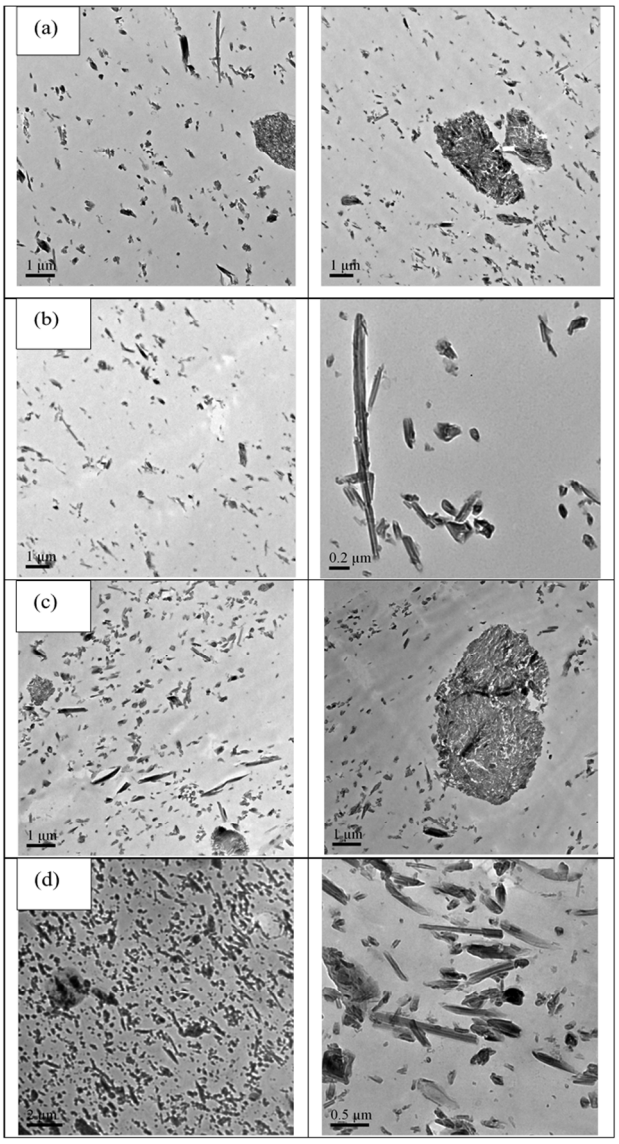

Figure 4: TEM micrographs of (a) PLA-H8, (b) PLA-H8-W, (c) PLA-H17 and (d) PLA-H17-W

Finally, structural characterization was performed by means of WAXS. Integrated intensity profiles computed from the 2D WAXS patterns are reported in figure 5.

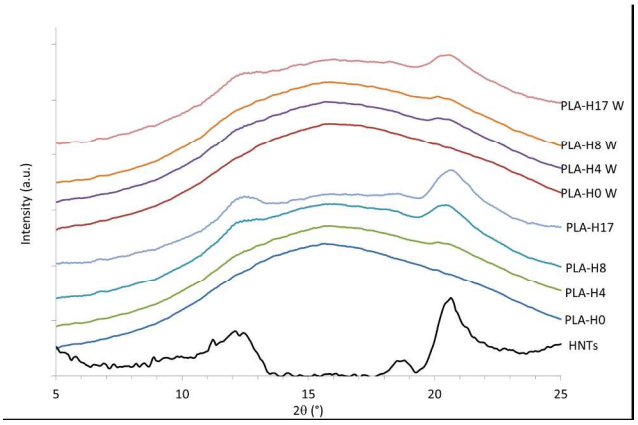

Figure 5: Integrated intensity profiles of PLA and its nanocomposites

Regarding to the filler, HNTs exhibits two main diffraction peaks at 2θ = 12.5° and 2θ = 20.5° assigned to the diffraction of d_{hkl} diffraction planes. Unfilled materials both exhibit a broad diffusion scattering and no diffraction peaks indicating the amorphous character of the neat materials. For the nanocomposites a broad diffusion scattering characteristic of an amorphous material is also observed whatever the clay content and the process used. Indeed the two peaks at 2θ = 12.5° and 2θ = 20.5°, visible on the intensity profiles, are attributed to the diffraction from HNTs and are not relevant of any crystalline phase of PLA. In summary all the materials of this study are amorphous.

Rheological properties

The storage modulus (G') and complex viscosity (η*) of neat PLA and its nanocomposites prepared with or without water injection are logarithmically plotted as a function of angular frequency in Figures 6a and 6b, respectively. At the measuring temperature of 180 °C and in the frequency range of 10^{-2} - 10^{2} rad/s, the pure polymer exhibits a Newtonian behaviour characterized by a slope of 2 for G' (i.e. G' ∝ ω²) and a plateau for η* in the low frequency region. On the contrary, no terminal regime is observed for the nanocomposites at low frequencies, even at the lowest filler concentration (4wt% HNTs). G' increases with increasing clay fraction and a plateau is observed starting from 17wt% HNTs. This latter indicates a transition from a liquid-like to a solid-like behaviour resulting from the formation of a percolated network structure wherein interactions between well-dispersed nanotubes start to dominate the relaxation process[29,48]. Moreover it is well-known that the

viscoelastic properties of composites at high frequencies are directly related to the polymer terminal relaxation and hence to the molecular weight of macromolecules[29].

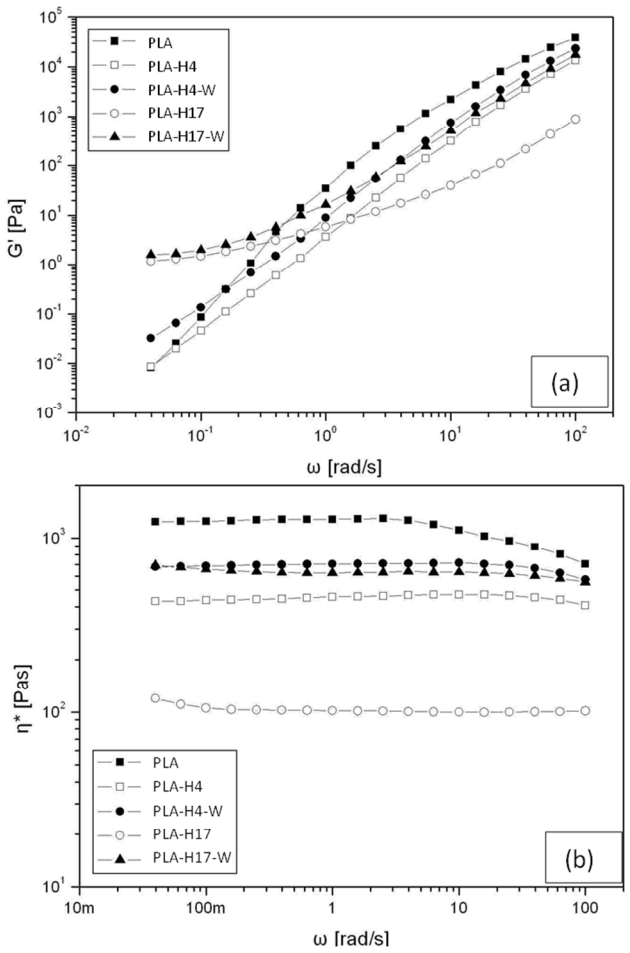

Figure6: (a) storage modulus (G') and (b) complex viscosity (η*) at 180°C as a function of frequency for PLA nanocomposites elaborated with and without water injection.

Compared to neat PLA, nanocomposites show lower moduli and viscosity at high frequencies associated to shorter relaxation times of polymer chains, especially for the highly loaded conventional formulations elaborated without water. This observation is in good agreement with results obtained from SEC measurements, confirming that the hydrolysis of PLA can be effectively prevented only when combining water injection and HNTs.

Thermomechanical properties

Thermal properties of the nanocomposites have been analyzed by means of DSC. Thermograms recorded upon 2nd heating for PLA and its nanocomposites extruded with and without water are reported in figure 7.

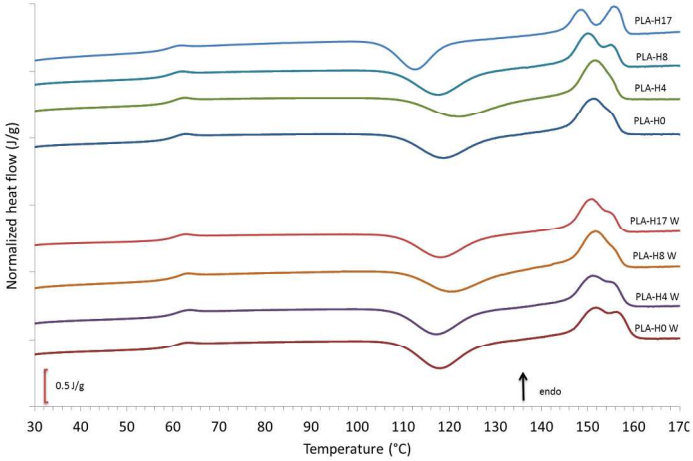

Figure 7: DSC thermograms of PLA and its nanocomposites extruded with and without water as a function of HNTs content

Upon heating a cold-crystallization occurs in the 110°C-130°C temperature range followed by a double melting peak around 155°C. This double melting peak has already been reported in the case of PLA and is ascribed to a phase transformation phenomenon. Indeed below 120°C it is the defective α' crystalline form that is induced and around 150°C this phase melts and transforms into the α stable crystalline form[49]. Calculations of the initial crystallinity show that all the samples were initially amorphous, confirming the WAXS results.

Nucleating effect of the filler was assessed by the study of isothermal crystallization kinetics. Figure 8 reports the crystallinity evolutions as a function of time for PLA-H0-W and PLA-H17-W samples isothermally crystallized at T = 110°C.

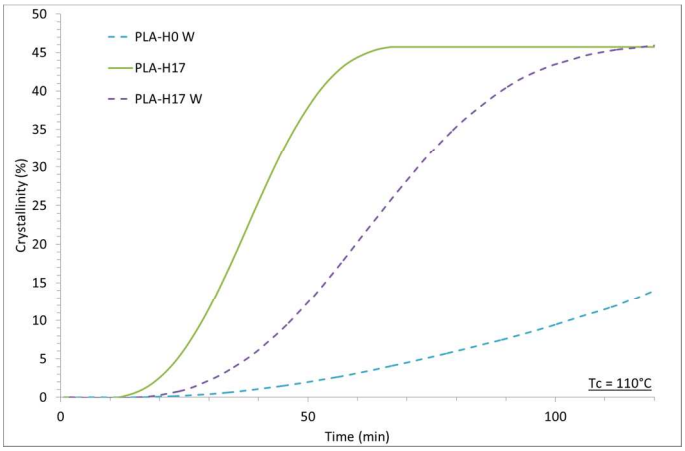

Figure 8: Isothermal crystallization kinetics at Tc = 110°C of PLA-H0 and PLA-H17-W nanocomposites.

It appears that nanocomposites exhibit faster crystallization kinetics than the unfilled sample. Indeed while the half crystallization time $t_{1/2}$ is reached after 60min and 30min for PLA-H17-W and PLA-H17 respectively, half of the crystallization is not reached after 120min for the PLA-H0-W sample. This demonstrates the nucleating effect of the HNTs on the PLA crystallization. Furthermore the faster crystallization kinetics of the PLA-H17 sample as compared to that of the PLA-H17-W sample can be ascribed to the lower molecular weight of the sample extruded without water injection.

A particular interest has also been paid to follow the evolution of the glass transition temperature (Tg). The values of Tg for the different materials, calculated from the DSC thermograms, are reported in Figure 9.

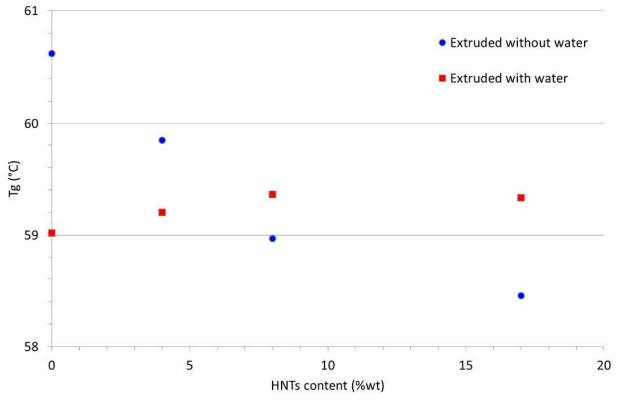

Figure 9: Evolution of Tg as a function of the HNTs content for nanocomposites extruded with and without water

In the case of water assisted extrusion Tg remains almost constant with increasing the clay content while Tg decreases with increasing the HNTs content for the materials elaborated without water injection. It is worth noticing that the same kind of behavior was observed for the evolution of the molecular weight. Consequently it is assumed that the evolutions of the glass transition temperatures are linked to the evolution of the molecular weights. In other words it seems that the values of Tg are not directly influenced by the HNTs content but rather by the degradation induced by processing without water injection and in the presence of filler. The fact that Tg is not significantly sensitive to the presence of the filler, even at high clay contents, has ever been reported in the case of PLA nanocomposites[50,51]. This can be interpreted by the fact that there are few interactions between the filler and the polymer matrix.

Mechanical behavior

Mechanical properties of the nanocomposites were determined from the tensile tests carried out at room temperature. Corresponding results are reported in table II.

Process	No water injection			Water injection		
Clay content (wt%)	0	4	8	0	4	8
E (GPa ±0.1)	2.1	2.2	2.4	2.2	2.25	2.45
Strain at break (% ±1)	7	6	6	6	6	5
Yield Stress (MPa ±0.1)	69	61	61	62	63	63

Table II: Mechanical properties of PLA and its nanocomposites at room temperature.

Regarding the evolution of the Young's modulus (E), a slight increase is observed when filler is added. E increases of 14% when 8wt% of HNTs are added. In the meantime the yield stress remains constant whatever the clay content and the processing route used. Finally, regarding the strain at break (ε_{break}), there are no significant changes when filler is added as PLA remains brittle whatever the case. The increase of E observed in this study is comparable with those reported by

other authors who used untreated HNTs [50,52] and slightly lower than those reported by authors using surface treated clays [31, 54].

Results reported in the literature indicate that in addition to improving the dispersion degree of the HNTs into the polymer matrix, a surface treatment of the HNTs also improves the interface between the nanotubes and the PLA matrix. Thus the fact that just a slight increase of mechanical properties is observed may arise from the non-organomodification of the HNTs surface. Indeed DSC results previously discussed suggest few interactions between the filler and the matrix

Moreover it appears that this rigidity increase is relatively low as compared to the morphology of the nanocomposites that is nearly exfoliated. The main reason to explain this result is that HNTs, due to their particular cylindrical structure, have a fairly lower weight/specific area ratio as compared to platelet like fillers such as Cloisite or Montmorillonite (MMT). Indeed while the specific area of MMT is about 600-700 m²/g, the specific area of HNTs is around 60m²/g, i.e. about 10 times lower. Taking into account that this specific area is a key parameter that will govern the gain, in terms of mechanical properties, the moderate enhancement of mechanical properties observed in this study has to be relativized. As an example, in the case of exfoliated nanocomposites, a HNTs content of 10wt% is equivalent to 1wt% of MMT in terms of specific area.

Thermal stability

Thermal stability of neat PLA and its nanocomposites was investigated by TGA analysis. Figure 10 presents TGA curves of the different samples under nitrogen at a heating rate of 10°C/min and the inset table summarizes the respective onset decomposition temperatures (T10). The thermal degradation of PLA is widely documented in the literature and takes place primarily through intramolecular trans-esterification with the formation of the monomer unit (i.e. lactide), but also cyclic oligomers, acetaldehyde, ketene, carbon dioxide and carbon monoxide[53]. As it can be seen from Figure 10, the thermal stability of PLA decreases monotonically with increasing clay content regardless of the elaboration conditions used. As an example, T10 drops from 343°C for neat PLA to 328°C and 327 °C when 8wt% of HNTs are added, without or with water injection respectively. This observation may be ascribed to a catalytic action of halloysite on the pyrolysis of PLA due to the presence of Brönsted acid sites (i.e. Si-OH and Al-OH) on the external surface of the clay. Such catalytic effect of clay nanoparticles has already been discussed in the literature for the thermal degradation of PLA[54] and polypropylene[55,56].

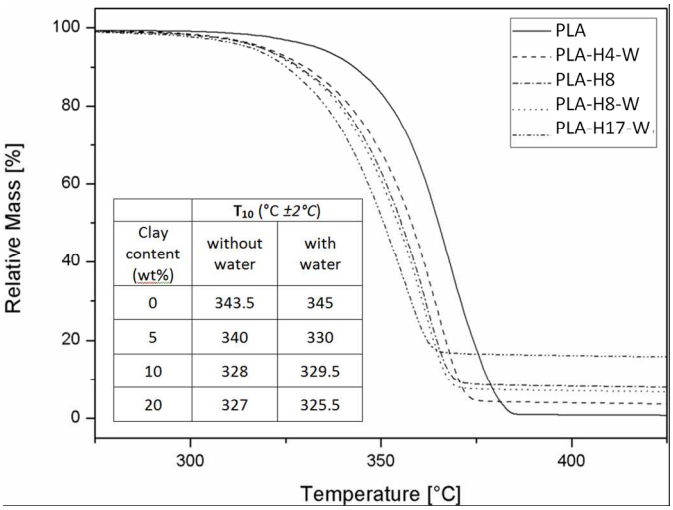

Clay content (wt%)	T_{10} (°C ±2°C) without water	with water
0	343.5	345
5	340	330
10	328	329.5
20	327	325.5

Figure 10: TG curves of neat PLA and its nanocomposites. The inset table summarize the onset decomposition temperature (T10) of the different samples

Fire performance

The small-scale mass loss calorimeter was used to evaluate the role of halloysite on the flammability of PLA. HRR curves for reference and nanocomposites are shown in Figure 11. The time to ignition (TTI), peak of heat release rate (pHRR), time to pHRR, total heat released (THR) and mass fraction of the residue are gathered in Table III. The TTI does not seem to be affected by the presence of the aluminosilicate nanotubes, while the pHRR decreases continuously with increasing clay fraction. Moreover, a further reduction in the pHRR is achieved by using water-assisted extrusion. As an example, the incorporation of 17wt% HNTs in PLA reduces the pHRR by about 29% and 43%, respectively, for samples prepared without and with water injection. This result is consistent with the structural investigation which highlights a beneficial effect of water on the clay dispersion (it was previously shown that high nanodispersion improves the fire performance of the material). The slight reduction of THR for nanocomposites may be ascribed to a dilution effect of the clay since the relative decrease in THR and the mass of the cone calorimeter residues

correspond approximately to the initial inorganic content in the PLA matrix[57].

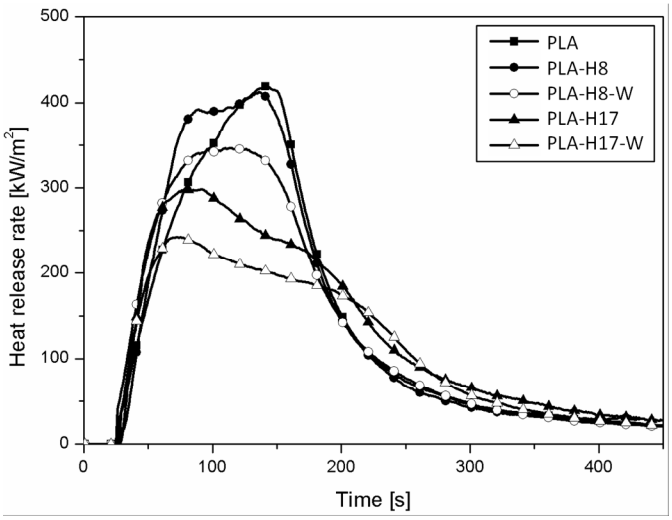

Figure 11: Heat release rate as a function of time for virgin PLA and different composite formulations (external heat flux = 50 kW/m²).

Samples	TTI[a] [s]	pHRR [kW/m²]	Time pHRR [s]	THR [MJ/m²]	Residue [wt%] (±1)
PLA	29 ±2	419	141	60	0
PLA-H8	28 ±1	413	136	61.5	8.4
PLA-H8 W	26 ±1	346	114	58.5	8.8
PLA-H16	28 ±1	298	78	56	17.1
PLA-H16 W	27 ±2	242	73	49.5	17.3

[a] TTI – time to ignition was defined as the time at which the HRR first increased to 25 kW/m².

Table III: Cone calorimeter data of neat PLA and its nanocomposites prepared with or without water injection. Tests were conducted at a heat flux of 50 kW/m².

The mode of action of HNTs as flame retardant additives has already been detailed in a previous work as a combination of physical processes taking place in the condensed phase and including barrier, heat sink and fuel dilution effects[58]. First, the presence of HNTs in the organic matrix enables the formation of an inorganic-rich layer at the sample surface during combustion through a combination of ablative reassembling of the nanotubes. This latter shield the underlying material from the external environment and limits the mass transport between condensed and gas phases. Second, the endothermic decomposition of halloysite absorbs a part of the external heat keeping the surrounding material cooler, but also dilutes the fuel concentration through the release of water vapour. However, the cooling and dilution effects of HNTs are believed to contribute to a lesser extent to the flame retardancy of polymeric materials due to the far lower global energy required by their endothermic transitions compared to conventional metal hydroxides[52].

Figure 12 presents the residue aspect of PLA-H-W nanocomposites after the cone calorimeter test. At low and intermediate clay concentrations (Fig. 12a), an inhomogeneous layer is formed at the surface of the condensed phase during burning. This latter, characterized by a combination of grey island-like floccules surrounded by uncovered areas, results from the bursting of gas bubbles at the sample surface, propelling the accumulated nanotubes outward from the bursting zone[51]. The size of the protective floccules increases progressively with increasing clay fraction, leading to the formation of a uniform inorganic layer covering the entire sample surface at 17wt% HNTs (Fig. 12b). The structural integrity of the protective layer is well preserved during combustion with only few cracks observed under the pressure exerted by volatile decomposition products. Therefore, the high effectiveness of the inorganic layer may be ascribed to its good barrier properties slowing down the escape of flammable volatiles, and hence reducing the flame intensity (i.e. pHRR).

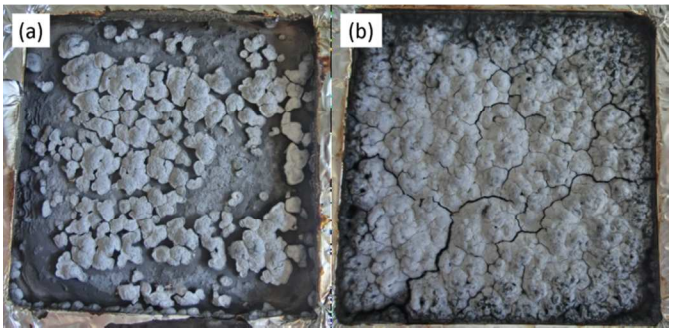

Figure 12: Cone calorimeter residues of: (a) PLA-H8-W and (b) PLA-H17-W nanocomposites.

Discussion

It was shown that using the water assisted extrusion process has a positive effect on the dispersion of the HNTs into the PLA matrix resulting in improved performance materials. This is particularly highlighted regarding the fire performance of the materials that are clearly better for the nanocomposites elaborated with water as compared to the ones elaborated via the conventional route. Another not expected effect of using the water assisted extrusion process pointed out in this study is that it prevents thermomechanical degradation of PLA. A similar effect was observed in the case of a copolyetheramide copolymer[59].

More precisely the thermodegradation effect encountered in the presence of HNTs in the case of conventional extrusion doesn't occur if water is added. Otherwise when no HNT's are added the presence of water involves a degradation of the PLA chains. Thus it seems that even if water involves an "expected" degradation of PLA when extruded alone, this negative effect is inhibited by the presence of HNTs. To explain this point it can be assumed that water molecules preferentially locate at the interface between the polymer and the HNTs. This preferential location arises from the high hydrophobicity of the surface of the HNTs due to permanent negative charges which exerts an attractive effect on the water molecules. This leads to the formation of hydrogen bonds[61].

The first implication of this is that water molecules are trapped onto the HNTs surface. This preferential location of water molecules can even lead to create a kind of phase separation between, on the one hand HNT surrounded by water and, on the other hand, neat PLA, hence avoiding molecular contact between water and PLA.

As a consequence, a first possible explanation of the observed "stabilization" phenomenon is of mechanochemical origin. It can be assumed that this "water-rich " second phase, including the HNTs, exerts a lubricant effect. This implies a decrease of the local shear stress concentration around the nanotubes that prevents mechanocissions of PLA chains. Such a lubrication phenomenon was already observed in the case of block copolymers leading to less degradation[60].

A second possible explanation is of chemical origin. As demonstrated by de Jong et al. the hydrolysis of PLA is strongly dependent on the pH of the medium, with a minimum degradation rate at pH around 4.5[60]. While at more acidic pH, the PLA degrades by acid-catalyzed ester hydrolysis, meaning polymer chain random scission, at pH above 4.5, it degrades by cyclization at polymer end groups ("back-biting") with elimination of lactide cyclic dimer leading to a kind of depolymerization (unzipping). The first random mechanism leads to a fast molecular mass decrease with the production of acid end-groups by hydrolysis, while the second one does not. Hence, it can be suggested that the presence of HNT somewhat stabilizes the pH on the "back-biting" side and limits the random chain scission of PLA by ester hydrolysis. Finally another possible consequence of the presence of water molecules is that, by forming H-bonds with HNT's surface, water molecules transform the Lewis acid sites present onto the surface into Brönsted ones, the catalytic effect of the latter on PLA hydrolysis being lower than the former ones.

Conclusions

The present study focused on the characterization of PLA/HNTs nanocomposites elaborated by means of water-assisted extrusion. Morphology characterization revealed that the injection of water during the extrusion has a benefiting effect on the dispersion degree of the clays even for HNTs contents as high as 17wt% where a nearly fully exfoliated morphology is observed. Besides even if untreated HNTs were used, dispersion degrees comparable to the ones observed in the case of surface treated HNTs are reached. This shows that

water assisted extrusion eliminates need for organomodification of clays.

Moreover it was shown that even if HNTs are well dispersed into the PLA matrix, only a moderate increase of mechanical properties was observed. This was ascribed to the lower specific area of HNTs as compared to more conventional fillers having a platelet shape. However, fire performance of PLA was significantly improved with the addition of HNTs and is explained by the formation of an inorganic layer at the surface of the sample. Finally, a key point of this study is that the injection of water during the extrusion of nanocomposites allows keeping the molecular weight of PLA constant with adding HNTs while a significant decrease of this parameter is observed in the case of conventional extrusion. Besides it seems that the injection of water inhibits the thermal degradation process of the macromolecular chains. This positive effect of injecting water was discussed and ascribed to a preferential location of the water molecules at the surface of the HNTs leading to a kind of phase separation.

Acknowledgements

Financial support from Région Nord Pas de Calais and European FEDER for SAXS-WAXS laboratory equipment is gratefully acknowledged. The SEM and TEM facility in Lille (France) is supported by the Conseil Regional du Nord-Pas de Calais, and the European Regional Development Fund (ERDF).

Notes and references

[a] Unité Matériaux Et Transformations, CNRS UMR 8207, Université de Lille1, ENSCL, Cité Scientifique, Bâtiment C6, 59655 Villeneuve d'Ascq, France

[b] Bio-and Soft Matter (BSMA), Institute of Condensed Matter and Nanosciences (IMCN), Université catholique de Louvain (UCL), Croix du Sud 1, Box 4, B-1348 Louvain-la-Neuve, Belgium

[c] SABIC T&I STC Geleen, Urmonderbaan 22,6167 RD Geleen, The Netherlands.

[d] Centre de ressources technologiques en chimie (Certech), rue Jules Bordet, Zone Industrielle C, B-7180 Seneffe, Belgium

[1] J. Lunt, *Polymer Degradation and Stability*, 1998, **59**, 145
[2] R.H. Wehrenberg, *Materials Engineering*, 1981, **94**, 63
[3] R.E. Drumright, P.R. Gruber, D.E. Henton, *Advanced Materials*, 2002, **12**, 1841
[4] E.S. Lipinsky, R.G. Sinclair, *Chemical Engineering Progress*, 1986, **82**, 26
[5] R. Auras, B. Harte, S. Selke, *Macromolecular Bioscience*, 2004, **4**, 835
[6] G. Kim, D. Lee, B. Hoffmann, J. Kressler, G. Stöppelmann, *Polymer*, 2001, **42**, 1095
[7] Y. Kojima, A. Usuki, M. Kawasumi, A. Okada, T. Kurauchi, O. Kamigaito, *Journal of Applied Polymer Science*, 1993, **49**, 1259
[8] J.W. Gilman, Applied Clay Science, 1999, **15**, 31
[9] L.J. Mathias, R.D. Davis, W.L. Jarrett, *Macromolecules*, 1999, **32**, 7958
[10] S. Sinha Ray, M. Okamoto, *Macromolecular Rapid Communications*, 2003, **24**, 815
[11] W. Chiu, Y. Chang, H. Kuo, M. Lin, H. Wen, *Journal of Applied Polymer Science*, 2008, **108**, 3024
[12] Hata, Isamu. J.P., Patent No. 2006335929
[13] S. Li, H. Yuan, T. Yu, W. Yuan, J. Ren, *Polymers for Advanced Technologies*, 2009, **20**, 1114
[14] J. Zhan, L. Song, S. Nie, Y. Hu, *Polymer Degradation and Stability*, 2009, **94**, 291
[15] M. Murariu, L. Bonnaud, P. Yoann, G. Fontaine, S. Bourbigot, P. Dubois, *Polymer Degradation and Stability*, 2010, **95**, 374
[16] M. Murariu, A.L. Dechief, L. Bonnaud, Y. Paint, A. Gallos, G. Fontaine, P. Dubois, *Polymer Degradation and Stability*, 2010, **95**, 889
[17] E. Joussein, S. Petit, J. Churchman, B. Theng, D. Righi, B. Delvaux, *Clay Minerals*, 2005, **40**, 383
[18] B. Lecouvet, J. Horion, C. D'Haese, C. Bailly, B. Nysten, Nanotechnology, 2013, **24**, art n°105704
[19] R.L. Frost, H.F. Shurvell, *Clays and clay Minerals*, 1997, **45**, 68
[20] M. Du, B. Guo, X. Cai, Z. Jia, M. Liu, D. Jia, *e-Polymers*, 2008, **130**, 1
[21] N.Y. Ning, Q.J. Yin, F. Luo, Q. Zhang, R. Du, Q. Fu, *Polymer*, 2007, **48**, 7374
[22] M. Liu, B. Guo, M. Du, Y. Lei, D. Jia, *Journal of Polymer Research*, 2008, **15**, 205
[23] H. Ismail, P. Pasbakhsh, M.N.A. Fauzi, A. Bakar, *Polymer Testing*, 2008, **27**, 841
[24] U.A. Handge, K. Hedicke-Höchstötter, V. Altstädt, *Polymer*, 2010, **51**, 2690
[25] B. Guo, .Q Zou, Y. Lei, D. Jia, *Polymer Journal*, 2009, **41**, 835
[26] K. Hedicke-Höchstötter, G.T. Lim, V. Altstädt, *Composite Science and Technology*, 2009, **69**, 330
[27] M. Murariu, A. Dechief, Y. Paint, S. Peeterbroeck, L. Bonnaud, P. Dubois P., *Journal of Polymers and the Environment*, 2012, **20**, 932
[28] M. Liu, Y. Zhang, C. Zhou, *Applied Clay Science*, 2013, **75**, 52
[29] K. Prashantha, B. Lecouvet, M. Sclavons, M.F. Lacrampe, P. Krawczak *Journal of Applied Polymer Science*, 2013, **128**, 1895
[30] W. Wu, X. Cao, Y. Zhang, G. He, *Journal of Applied Polymer Science*, 2013, **130**, 443
[31] W.S. Chow, W.L. Tham, P.C. Seow, *Journal of Thermoplastic Composite Materials*, 2013, **26**, 1349
[32] P. Russo, S. Cammarano, E. Bilotti, T. Peijs, P. Cerruti, D. Acierno, *Journal of Applied Polymer Science*, 2014, **131**, 39798
[33] G. Gorrasi, R. Pantani, M. Murariu, P. Dubois, *Macromolecular Materials and Engineering*, 2014, **299**, 104

[34] B. Lecouvet, M. Sclavons, C. Bailly, S. Bourbigot, *Polymer Degradation and Stability*, 2013, In Press
[35] B. Lecouvet, M. Sclavons, S. Bourbigot, J. Devaux, C. Bailly, *Polymer*, 2011, **52**, 4284
[36] D. Rousseaux, N. Sallem-Idrissi, A.C. Baudouin, J. Devaux, P. Godard, J. Marchand-Brynaert, M. Sclavons, *Polymer*, 2011, **52**, 443
[37] F. Touchaleaume, J. Soulestin, M. Sclavons, J. Devaux, M.F. Lacrampe, P. Krawczak, *Polymer Degradation and Stability*, 2011, **96**, 1890
[38] G. Stoclet, M. Sclavons, J. Devaux, *Journal of Applied Polymer Science*, 2013, **127**, 4809
[39] B. Lecouvet, J.G. Gutierrez, M. Sclavons, C. Bailly, *Polymer Degradation and Stability*, 2011, **96**, 226
[40] N. Fedullo, M. Sclavons, C. Bailly, J.M. Lefebvre, J. Devaux, *Macromolecular Symposia*, 2006, **233**, 235
[41] N. Fedullo, E. Sorlier, M. Sclavons, C. Bailly, J.M. Lefebvre, J. Devaux, *Progress in Organic Coatings*, 2007, **58**, 87
[42] E.W. Fischer, H.J. Sterzel, G. Xegner, *Colloid Polymer and Science*, 1972, **251**, 980
[43] G. Perego, G.D. Cella, C. Bastioli, *Journal of Applied Polymer Science*, 1996, **59**, 37
[44] F. Carrasco, P. Pagès, J. Gámez-Pérez, O.O. Santana, M.L. Maspoch, *Polymer Degradation and Stability*, 2010, **95**, 116
[45] Q. Zhou, M. Xanthos, *Polymer Degradation and Stability*, 2009, **94**, 327
[46] R. Scaffaro, L. Botta, E. Passaglia, W. Oberhauser, M. Frediani, L. Di Landro, *Polymer Engineering and Science*, 2013, In Press
[47] S. Li, *Journal of Biomedical Materials Research*, 1999, **48**, 342
[48] A.J. Hsieh, P. Moy, F.L. Beyer, P. Madison, E. Napadensky, J. Ren, R. Krishnamoorti, *Polymer Engineering and Science*, 2004, **44**, 825
[49] J. Zhang, K. Tashiro, H. Tsuji, A.J. Domb, *Macromolecules*, 2008, **41**, 1352
[50] D. Wu, L. Wu, L. Wu, B. Xu, Y. Zhang, M. Zhang, *Journal of Polymer Science, Part B: Polymer Physics*, 2007, **45**, 1100
[51] Q.K. Meng, M. Hetzer, D. De Kee, *Journal of Composite Materials*, 2011, **45**, 1145
[52] K. Prashantha, B. Lecouvet, M. Sclavons, M.F. Lacrampe, P. Krawczak, *Journal of Applied Polymer Science*, 2013, **128**, 1895
[53] F.D. Hopinke, K. Mackenzie, *Journal of Analytical and Applied Pyrolysis*, 1997, **40**, 43
[54] T.D. Hapuarachchi, T. Peijs, *Composites: Part A*, 2010, **41**, 954
[55] A. Marcilla, A. Gomez, S. Menargues, R. Ruiz, *Polymer Degradation and Stability*, 2005, **88**, 456
[56] G. Tartaglione, D. Tabuani, G. Camino, M. Moisio, *Composites Science and Technology*, 2008, **68**, 451
[57] T. Kashiwagi, R.H. Harris Jr., X. Zhang, R.M. Briber, B.H. Cipriano, S.R. Raghavan, W.H. Awad, J.R. Shields, *Polymer*, 2004, **45**, 881
[58] B. Lecouvet, M. Sclavons, S. Bourbigot, C. Bailly, *Polymers for Advanced Technologies*, 2014, **27**, 137
[59] F. Touchaleaume, J. Devaux, P. Krawczak, M. Sclavons, J. Soulestin, F. Malet, N. Dufaure, J.J. Flat, Demande de Brevet Français FR1061274 27 Décembre 2010 –PCT/FR2011/053186 du 23/12/11
[60] S.J. De Jong, E.R. Arias, D.T.S. Rijkers, C.F. Van Nostrum, J.J. Kettenes-Van den Bosch, W.E. Hennink, *Polymer*, 2001, **42**, 2795

